Marine Chemistry 267 (2024) 104465

Contents lists available at ScienceDirect

Marine Chemistry

journal homepage: www.elsevier.com/locate/marchem

Reactivity and fluxes of antimony in a macrotidal estuarine salinity gradient: Insights from single and triple quadrupole ICP-MS performances

Teba Gil-Díaz [a,b,*], Frédérique Pougnet [a], Lionel Dutruch [a,1], Jörg Schäfer [a], Alexandra Coynel [a]

[a] Université de Bordeaux, UMR CNRS 5805 EPOC, Allée Geoffroy Saint-Hilaire, 33615 Pessac, France
[b] Institute of Applied Geosciences, Karlsruhe Institute of Technology, Adenauerring 20b, 76131 Karlsruhe, Germany

ARTICLE INFO

Keywords:
QQQ-ICP-MS
UV-oxidation
Dissolved net flux
Gironde estuary

ABSTRACT

Trace element analyses in brackish waters are challenging for many elements at ppb/ppt levels and analytical methods. In this work, we compare two methods using inductively coupled plasma mass spectrometry (ICP-MS) for quantifying antimony (Sb). Results of a previous study along the salinity gradient in a macrotidal estuary (i.e., the Gironde Estuary, France) using isotopic dilution via single quadrupole ICP-MS are compared to reanalyzed aliquots of the same samples. Direct analyses of estuarine water samples via standard additions ($N = 52$) were performed with a QQQ-ICP-MS (new generation, iCAP TQ Thermo®) to determine dissolved (< 0.2 μm filtered and UV-irradiated replicates) Sb concentrations during two contrasting hydrological conditions (low vs high freshwater discharges). Despite following good analytical practices on both studies, the use of the new analytical device provides more robust results and highlighted a characteristic ^{121}Sb isotopic interference in estuarine samples at S > 20, efficiently eliminated by the QQQ-ICP-MS performance. This means that Sb reactivity shows an additive, non-conservative behavior in the Gironde Estuary, with a more defined bell-shaped profile in low discharge compared to high discharge conditions. This approach allows to quantify for the first time in the literature Sb dissolved net fluxes from the Gironde Estuary to the Atlantic coast and provides an updated value for the seawater endmember. This study opens future applications of QQQ-ICP-MS for quantifying on a more routine basis dissolved trace elements in brackish waters, providing guidelines and good practices for field studies regarding Sb determination in estuarine systems.

1. Introduction

Antimony (Sb) is a metalloid, classified by the EU as a Critical Raw Material with moderate risk supply for technological development (European Commission (EU COM474), 2020). Due to its toxicity, Sb is also present in European lists of relevant substances (French Prefectural Order of June 30th 2005) and in worldwide lists of pollutants of priority interest (European Council (EC), 2006; DFG (Deutsche Forschungsgemeinschaft), 2023; USEPA, 2013). Despite its unknown biological functions (Tamás, 2016), Sb is easily accumulated in aquatic organisms (e.g., Filella et al., 2007; Guérin et al., 2011). However, it is hardly possible to evaluate the risk of Sb transfer to organisms in brackish/seawater environments given the lack of reported dissolved Sb concentrations and the reliability of the values in saline water matrices (Filella et al., 2007). The intrinsic challenges related to the analyses of brackish/saline water matrices are also one of the reasons why Sb behavior, transport and fluxes (i.e., net vs gross) in continent-ocean transition systems is still not well characterized/known. Accurate and reliable flux calculations are fundamental for quantifying the transport of trace elements between environmental compartments/reservoirs. These calculations help determine system resilience regarding natural vs anthropogenic mass budgets (i.e., pertinent in estuaries given their multiple ecosystem functions, Pougnet et al., not published), and characterize/model the biogeochemical cycle of trace elements (i.e., still unknown or under/overestimated for the case of Sb due to lack of data, e.g., Fu et al., 2023, Mitra and Sen, 2017, Wu et al., 2008).

Reported Sb dissolved concentrations of the seawater endmember since the 1960's was highly variable (i.e., ranging between ~0.2–4.1 nM, ~20–500 ng L^{-1}) until ~1985, when concentrations started to be somewhat consistent with the upcoming of ICP-MS techniques (i.e., average concentrations of 1.51 ± 0.37 nM, 184 ± 45 ng L^{-1}; Filella et al., 2002a). The few existing studies ($N = 9$) in estuarine systems that

* Corresponding author at: Institute of Applied Geosciences, Karlsruhe Institute of Technology, Adenauerring 20b, 76131 Karlsruhe, Germany.
E-mail address: teba.gil-diaz@kit.edu (T. Gil-Díaz).
[1] Present address: Université de Rennes, UMR CNRS 6118, Campus Beaulieu 35000 Rennes, France.

https://doi.org/10.1016/j.marchem.2024.104465
Received 30 April 2024; Received in revised form 5 September 2024; Accepted 26 October 2024
Available online 28 October 2024

followed up, using contrasting techniques (e.g., Hydride Generation coupled to AAS or AFS, neutron activation analyses, Cathodic/Anodic Stripping Voltammetry, and ICP-MS), reported different reactivities of Sb along the salinity gradients of the studied systems (i.e., conservative and non-conservative behavior; Andreae et al., 1983, Byrd, 1990, Gil-Díaz et al., 2016, Salaün et al., 2012, van den Berg et al., 1991, van den Berg, 1993, van der Sloot et al., 1985, Wilson and Webster-Brown, 2009, Wu et al., 2011). In these studies, the number of estuaries that ended up at the average seawater endmember (i.e., Filella et al., 2002a) vary independently to the choice of the analytical technique. However, in lack of available certified materials for Sb in brackish/seawater matrices, it is surprising that no study until now has reanalyzed the same samples with different techniques to verify the accuracy and precision of their analytical approaches. Validating estuarine patterns of dissolved Sb would allow to reliably quantify daily export (net) fluxes of Sb to the coastal areas, something seldomly done in the studies published until now ($N = 2$; Andreae et al., 1983, Wilson and Webster-Brown, 2009).

Inductively coupled plasma – mass spectroscopy (ICP-MS) is generally the instrument of choice for routine analyses of environmental samples presenting trace to ultra-trace element concentrations (Zhu et al., 2021). There is a wide range of possibilities to analyze dissolved concentrations of trace elements in brackish/seawater samples with ICP-MS techniques. The overall challenges linked to analyzing samples with high salt content rely on multiple complications that might overweight the concentrations of the analyte of interest in the sample, affecting the quality of the data. For example, saline samples may generally clog the sample path (nebulizer, torch, cones, etc.) and cause analyte-specific effects such as decreased ionization efficiencies and increased spectral interferences. Therefore, the most common approach in many cases involves a pre-treatment step before the analyses, i.e., via co-precipitation (e.g., Zhu, 2020) or reducing the salt content (e.g., resins or sample dilution, Li et al., 2022, Siems et al., 2024), sometimes combined with further analytical methods/instrumental gadgets during the analyses (e.g., isotopic and gas dilution, Gil-Díaz et al., 2016) or with higher resolution techniques (e.g., SF-ICP-MS, Kuznetsova and Timerbaev, 2021). Among new generation analytical techniques (e.g., Balaram, 2021), the triple quadrupole ICP-MS (QQQ-ICP-MS) is probably the world's widely used mass spectrometer (Yost, 2022). For our purpose, it allows direct analysis of brackish water matrices due to its robust equipment and high sensitivity (Yost, 2022; Zhu et al., 2021), potentially compatible with trace to ultra-trace element concentrations in seawater environments. In addition, direct sample analysis reduces the potential biases from pre-concentration approaches, such as element loss or contamination. Nevertheless, this application is relatively recent and is under development, thus little experience and knowledge is available on one-to-one comparison with previous equipment, particularly for the case of Sb (e.g., Zhu et al., 2021).

Unless combined with pre-injection techniques (e.g., HG, HPLC, GC, etc.), analyses of water samples via ICP-MS are assumed to provide "total" or bulk trace element dissolved concentrations. That is, out of all Sb species (i.e., inorganic or organic, in the truly dissolved phase or in colloidal form, Andreae et al., 1981, Filella et al., 2002b, Caplette and Mestrot, 2021, Filella and Rodríguez-Murillo, 2021), when quantifying water at the ICP-MS one will obtain a concentration equivalent to the total sum of Sb species/forms. Furthermore, depending on the sampling approach, water samples can contain both "truly" dissolved and colloidal phases (i.e., determined by the filter mesh-size in field studies). This means that, apart from the dissolved species, Sb complexed with natural organic matter (NOM) can also be present in the sample, for which little is yet known regarding their relevance in Sb natural cycling and the associated analytical artifacts (Filella and Rodríguez-Murillo, 2021). However, to the best of our knowledge, nobody has verified if the presence of organic components in water samples causes any analyte loss during classical ICP-MS analyses, as observed for other elements like Sn (Pougnet et al., not published). Therefore, pre-treatments like UV-digestions (i.e., commonly used in voltammetry studies to avoid the presence of organic matter during the measurements, Abdou et al., 2020, van den Berg et al., 1991), can provide a simple insight to the proportion and influence of organic vs inorganic element species when analyzing aliquots of the same water sample (UV-treated and non-UV treated) via ICP-MS, even though the efficiency of the UV-digestion has not yet been demonstrated for the case of Sb (Filella and Rodríguez-Murillo, 2021).

This study aims at (i) comparing the analytical performance of the ICP-MS vs the QQQ-ICP-MS for dissolved Sb (Sb_d) concentrations in brackish and seawater matrices at the case study area of the Gironde Estuary (France) to reliably quantify Sb_d concentrations in challenging matrices, (ii) identifying the potential influence of organometallic Sb or Sb-NOM related species on total Sb_d quantification along the salinity gradient via direct vs UV-irradiated replicates of water samples, and (iii) quantifying for the first time for the Gironde Estuary the daily export (net) fluxes of Sb_d to the Atlantic Ocean. To achieve this, we compare water samples collected in the Gironde Estuary during contrasting hydrological conditions with nearby areas, independent from the estuarine influence. This approach will allow to establish reliable routine analyses to better understand the biogeochemical processes concerning Sb_d reactivity, advancing the knowledge of Sb dynamics in estuarine systems and providing a more reliable tool for risk assessment.

2. Experimental

2.1. Study sites

The Gironde Estuary is the largest macrotidal estuary in SW Europe with an important Maximum Turbidity Zone (MTZ, > 1 g L^{-1}). Estuarine water discharges are represented by freshwater inputs from the main rivers: Garonne, Dordogne and Isle (Fig. 1). In this study, water samples ($N = 93$ in total) were collected during four sampling campaigns (MGTS I in March 2014, MGTS II in March 2015, MGTS III in October 2015, and MGTS IV in June 2017, Fig. 1) on-board the R/V Thalia (IFREMER). The acronym of the sampling campaigns (i.e., MGTS) stands for "Métaux Gironde Transferts et Spéciation", i.e., metal transfers and speciation in the Gironde. These campaigns represent contrasting freshwater discharge conditions ranging from intermediate/high (1203 m^3 s^{-1} in MGTS I and 3450 m^3 s^{-1} in MGTS II) to low (248 m^3 s^{-1} in MGTS III and 235 m^3 s^{-1} in MGTS IV) discharges. They were performed along the salinity ($0 < S < 35$) and turbidity (18–12,000 mg L^{-1}) gradients of the

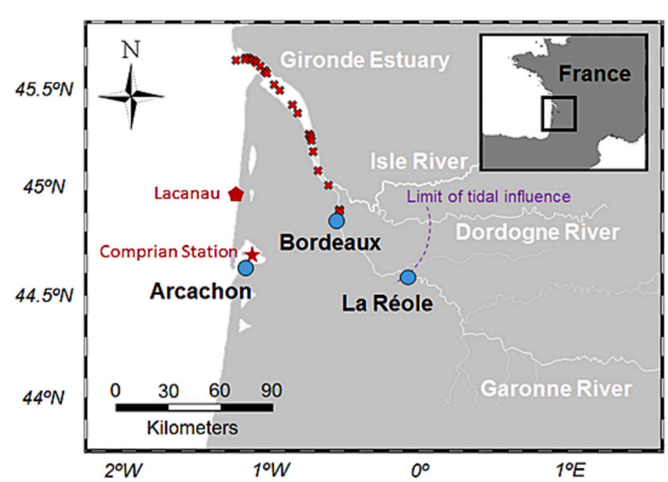

Fig. 1. Map of the Gironde Estuary (SW France). Main urban areas like Bordeaux, Arcachon and La Réole (filled circles) and river inputs to the Gironde Estuary (Garonne, Dordogne and Isle) are shown. Sampling points along the estuarine salinity and turbidity gradients (MGTS I-IV; crosses) and point sampling sites at Lacanau (pentagon) and Comprian station (star) from a previous study (Gil-Díaz et al., 2016) are also indicated.

Gironde Estuary, from the city of Bordeaux to the estuary mouth. These four sampling campaigns are the focus of this work. Nevertheless, additional samples from areas nearby the study site (i.e., point site at Lacanau collected in April 2016, also in the Atlantic coast but independent of the influence from the Gironde Estuary, and a 24 h cycle sample collection at Comprian in the Arcachon Bay in April 2015, presented in Fig. 1) are also included in this work to improve its robustness regarding Sb quantification.

2.2. Sample collection

During all sample campaigns, several parameters and samples were collected. Water was sampled using Niskin bottles at 1 m depth, immediately filtered onboard. For the case of Sb quantification, this water was filtered through 0.2 μm Minisart® cellulose acetate filters and collected into three replicates of 30 mL each in acid-washed polypropylene (PP) bottles. Samples were acidified with HNO_3 (1/1000 *v*/v; J.T. Baker ultrapure, 14 M) and stored at 4 °C in the dark until analysis. The water samples from the Gironde Estuary (MGTS I-IV) and Lacanau were distributed into aliquots and analyzed in multiple occasions (e.g., some already published in Gil-Díaz et al., 2016). A summary of all the samples used in this work (newly published data vs already published information) is presented in Table 1 for clarity. Table 1 also contains analytical information which will be described in the following section.

In addition to water collection, salinity was quantified with a TetraCon 96® probe (PROFILINE, WTW) and turbidity via suspended solid concentrations (i.e., filtration of known volumes of water in pre-weighed Xilab glass microfiber filters, 0.7 μm) as described in Gil-Díaz et al. (2016). Furthermore, Chlorophyll-a (Chl-a) and Phaeopigments (i.e., degradation products of Chl-a) were quantified from water aliquots in MGTS I and MGTS III (Pougnet, 2018). That is, depending on the water turbidity, known volumes of the water collected with the Niskin bottles were also filtered via 0.7 μm and Ø 47 mm Whatman® GF/F filters with a manual pump (i.e., to avoid cell destruction, as recommended in Pougnet, 2018). Filters were then wrapped in aluminum foil and immediately stored at −20 °C during sampling, then at −80 °C in the laboratory pending analyses (Billy et al., 2015). Though this data has already been published in Pougnet (2018), it is included in this work to help build the case for Sb observations.

2.3. Analyses

2.3.1. Dissolved Sb

In this work, dissolved Sb concentrations from the four MGTS sampling campaigns and from Lacanau were firstly analyzed directly, here labelled as non-UV-irradiated samples (Sb_x). That is, samples were analyzed by standard additions using monoelemental solutions (Sb SPEX CertiPrep 0.6 % Tart. Acid/Tr. HNO_3) and minimal sample dilution (i.e., factor 1.1). Quantification was performed with high matrix cones, argon gas dilution and kinetic energy dispersion (KED, He-based) mode at the QQQ-ICP-MS (iCAP TQ Thermo®). In the lack of estuarine or seawater certified reference materials (CRM) for Sb, a freshwater CRM (TMRAIN 23.4; $N = 2$) was used to verify the instrument methodology, obtaining good recoveries of 105 %. Analytical repeatability was followed-up at each analytical series ($N = 8$) with the coastal seawater sample from Lacanau, showing good precision with 9 % relative standard deviation (RSD). In addition, these analyses of Lacanau water were used to evaluate the instrument stability concerning direct matrix injection, obtaining immediate performing responses from the first analysis for Sb (10 % RSD). Field blanks ($N = 3$, Table 1) showed low onsite contamination and/or low filter influence (i.e., 0.2 μm Minisart® cellulose acetate) on dissolved Sb concentrations, showing average concentrations of 0.07 ± 0.08 nM (8.50 ± 9.20 ng L^{-1}). The complete raw data of the field blanks is shown in Table S1 (Supplementary data).

In addition to Sb_x, aliquots of the previously filtered and stored samples from Lacanau, MGTS I and III were subjected to UV-irradiation pretreatment, thus here called UV-irradiated samples (Sb_{tot}). For this, volumes (< 10 mL) from the PP bottles were transferred to acid-washed Teflon bottles, after rinsing three times with the sample. These replicates were left over night in a UV box (i.e., UV lamp of 254 nm and 40 W) and analyzed the day after following the QQQ-ICP-MS procedure for dissolved Sb quantification via standard additions. The duration of the UV irradiation on the samples is considered appropriate given that van den Berg et al. (1991) also applied successfully UV–photolysis to 50 mL sample volume for 4 h to analyze Sb in the Tamar Estuary. Blanks to account for potential contaminations from the UV-irradiation procedure ($N = 6$, Table 1) were prepared with ~10 mL of deionized water (Milli-Q® Millipore) and subjected to the UV-treatment in the Teflon bottles. Results showed relatively high variations of Sb concentrations, i.e., 0.15 ± 0.13 nM (18.8 ± 16.4 ng L^{-1}). The full raw dataset from the UV-treatment blanks is also shown in Table S1.

The obtained results from Sb_x and Sb_{tot} at the QQQ-ICP-MS will be

Table 1

Overview of the number and origin of the samples used in this work. The analytical instruments (QQQ-ICP-MS vs PC3-ICP-MS), quantification approaches (via standard additions or isotopic dilution - ID) and sample pre-treatment (UV-treated yes/no) are also presented, indicating the respective notations used along this work for the resulting dissolved Sb concentrations (Sb_{tot} vs Sb_x).

Campaigns (date)	N° original water samples	Analytical approach on aliquots of the original sample			
		QQQ-ICP-MS			(PC3)ICP-MS
		via standard additions		via ID	via ID
		with UV (Sb_{tot})[a]	no UV (Sb_x)[a]	no UV (Sb_x - ID)[a]	no UV (Sb_x)[b]
Milli-Q® Millipore[#]	6	6	–	–	–
Field blanks[+]	3	–	3	–	–
MGTS I (March 2014)[++]	24	24	24	24	24*
MGTS II (March 2015)	23	–	23	–	23**
MGTS III (October 2015)[++]	26	26	26	–	26*
MGTS IV (June 2017)	20	–	20	–	–
Lacanau – point site (April 2016)	3	1	1[x]	–	3[a]
Comprian – point site in the Arcachon Bay (April 2015)	26	–	–	–	26*

References: [a] This work, [b] Gil-Díaz et al., 2016, [c] Pougnet, 2018

Exceptions: *Only presented in the Supplementary information (Fig. S1), **Not shown in this work.

Clarifications: [#] UV-treatment blanks, [+] Milli-Q® Millipore water filtered onsite in the field, [++] In addition to water samples, corresponding concentrations of Chlorophyll-a[c] and Phaeopigments[c] are also included in this work, [x] Analyzed a total of 8 times for reproducibility, i.e., once with every batch of Sb analyses.

compared and discussed to previously quantified Sb_x aliquots of the same filtered and stored samples of MGTS I-III, Lacanau and Comprian (Table 1), analyzed and published in Gil-Díaz et al. (2016). The latter study quantified Sb from isohaline diluted samples through isotopic dilution (ID, Eq. (1) adapted from Castelle, 2008) with ^{123}Sb solution (99.43 % purity, Oakridge, USA) and Ar-gas dilution from external PC3 ESI system coupled to ICP-MS (X-Series Thermo®). To provide further insights on the comparison between the QQQ-ICP-MS and PC3-ICP-MS techniques, aliquots from MGTS I were further quantified via ID (as in Gil-Díaz et al., 2016) with the QQQ-ICP-MS (Table 1).

$$c = \frac{c_a \cdot w_a \cdot A_r \cdot (R \cdot X_a - Y_a)}{w \cdot A_{ra} \cdot (Y - R \cdot X)} \quad (1)$$

where c is the unknown concentration (total Sb in the sample, ng L^{-1}), c_a the concentration of Sb from the certified solution, w the mass or volume of sample aliquot, w_a the mass or volume from the certified solution, A_r the relative atomic mass of natural Sb (i.e., 121.9 g mol^{-1}) and A_{ra} that of the certified solution (i.e., 122.9 g mol^{-1}), being X/Y the relative abundance (%) of $^{123}Sb/^{121}Sb$ in the sample compared to that of X_a/Y_a in the certified solution (e.g., 99.43 % purity) and R the isotopic ratio measured at the ICP-MS.

2.3.2. Chlorophyll-a and Phaeopigments

Chlorophyll-a and Phaeopigment concentrations were quantified with a Turner Designs Trilogy Fluorometer and published in Pougnet (2018), thus will not be described in detail in this work. Briefly, the fluorometric analyses followed a modified method from Vernon (1960) and Yentsch and Menzel (1963), where the filters are submerged in acetone (90 %), gently ground, placed in the fridge for 18 h, and then centrifuged twice at 5 °C (4000 rpm). Chlorophyll-a was measured directly in an aliquot of the supernatant via red light emission (> 665 nm) after excitation on the blue light range (446–500 nm). Phaeopigments were measured similarly after acidification of the supernatant with HCl (0.3 M). Both parameters were quantified following the equations defined in Lorenzen (1967), as described in Pougnet (2018).

3. Results and discussion

3.1. Analytical performance of ICP-MS techniques

Analyses on dissolved Sb at the QQQ-ICP-MS showed a general bell-shaped trend along the salinity gradient, centered at mid-salinities, for both hydrological conditions and sample replicas (non-UV and UV-irradiated, as will be shown in Section 3.3.). Nevertheless, the same non-UV-irradiated samples from MGTS I, II and III previously analyzed in Gil-Díaz et al. (2016), showed a bell-shaped Sb maximum displaced towards high salinity ranges (e.g., Supplementary data Fig. S1a and b). A comparison between both ICP-MS techniques shows similar concentrations, of the same order of magnitude for most salinity ranges (e.g., Fig. 2), though resulting in different profiles along the salinity gradient (e.g., Fig. S1a and b). Only samples with S > 20 showed higher concentrations at the PC3-ICP-MS (Gil-Díaz et al., 2016). These results either suggest (i) a potential sorption of Sb_d onto storage bottle walls for S > 20 over time, or (ii) an Sb interference at the PC3-ICP-MS analysis, successfully eliminated by QQQ-ICP-MS (e.g., as proven by the ID measurement at the QQQ-ICP-MS for MGTS I, Sb_x - ID in Fig. 2). The former case is unlikely given the contrasting patterns during low discharge conditions (Fig. S1b), and the fact that Sb_d during drought conditions from the recent campaign in 2017 (MGTS IV), analyzed at the QQQ-ICP-MS, also showed reproducible bell-shaped trends like MGTS III (see Section 3.3.). The latter possibility could be explained by analytical variability (e.g., ± 15 % error, area within the dashed lines in Fig. 2) and/or other concurring potential interferences.

Given the nature of the ID procedure (i.e., spike with ^{123}Sb) an interference during ID quantification implies a spectral influence on ^{121}Sb, which is not related to the ionic strength per se (i.e., $^{40}Ar^{81}Br$) given the lower bias of the results from the seawater samples at Comprian Station in the Arcachon Bay measured with the PC3-ICP-MS (Table 1, Fig. S1). In addition, the concurring analytical interference seems to be site-dependent, i.e., detected only at the Gironde Estuary mouth. This is deduced from (i) the lower variability obtained for the Sb concentrations of Lacanau (PC3-ICP-MS vs QQQ-ICP-MS, Fig. S1) compared to the estuarine high salinity samples (MGTS I and III, Fig. S1), and (ii) the matching seawater trends between the water samples collected at Comprian Station and the estuarine trend of MGTS I via QQQ-ICP-MS (Fig. S1). In both cases, these coastal values (Lacanau, Comprian and reanalyzed samples for the MGTS series) are in accordance with average seawater Sb endmembers registered in the literature with ranges of 1.51 ± 0.37 nM (184 ± 45 ng L^{-1}, Filella et al., 2002a). Additional parameters such as SPM, Chl-a and phaeopigment concentrations could hint towards potential interferences related to variable biological activities or mineral loads, which differ between the Gironde Estuary mouth and the Arcachon Bay (Fig. S1c,d).

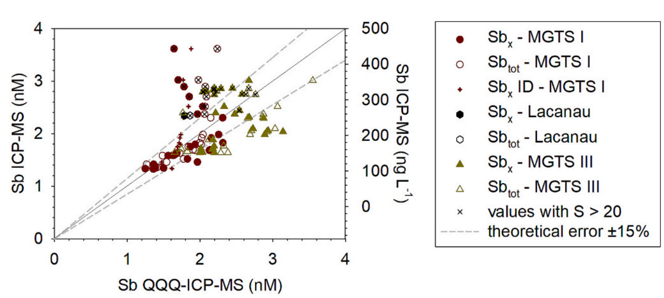

Fig. 2. Comparison between two analytical approaches quantifying Sb in brackish waters. Total Sb dissolved concentrations were measured by isotopic dilution (ID) in ICP-MS (Gil-Díaz et al., 2016) and by standard additions in QQQ-ICP-MS (this work) for the same samples and hydrological sampling conditions: intermediate (1203 $m^3 s^{-1}$ MGTS I, circles) and low (248 $m^3 s^{-1}$ MGTS III, triangles) freshwater discharges. The value from Lacanau is also included (hexagon), as well as MGTS I samples measured by ID at the QQQ-ICP-MS (plus signs). Values corresponding to S > 20 are marked with a cross over the corresponding symbol. The legend refers to the sample analyzed at the QQQ-ICP-MS, i.e., both non-UV-irradiated samples (Sb_x) and UV-irradiated replicates (Sb_{tot}).

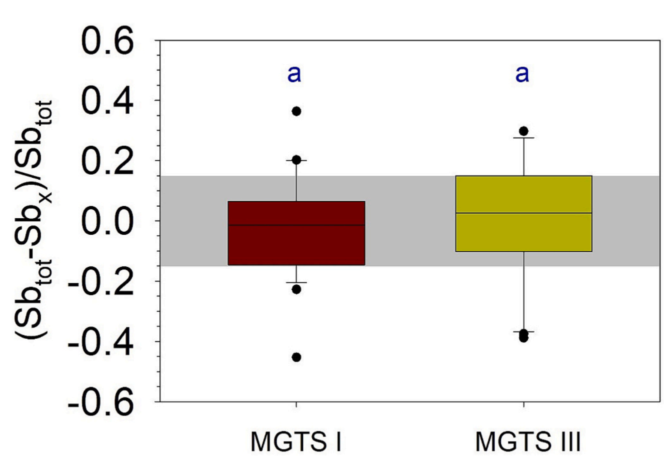

Fig. 3. Box-plots for the difference between Sb_{tot} and Sb_x in MGTS I and MGTS III. The median of each dataset is shown with a line. The grey area shows the range of ±15 % variability. Shapiro-Wilks and Levene's tests showed normal distributions (p_value = 0.26) and equal variances (p_value = 0.57) for both datasets. There is no significant difference between the averages of both datasets (p_value = 0.53 for *t*-test) and each mean is not significantly different to zero (p_values are 0.52 for MGTS I and 0.79 for MGTS III in one-sample *t*-tests, respectively). Statistical tests were obtained via IBM SPSS v20 and are shown in the graph with the letter a.

3.2. Dissolved species along the salinity gradient

In most cases, differences between non-UV and UV-irradiated samples along the salinity gradient averaged ±15 % during both MGTS I and MGTS III hydrological conditions (i.e., grey area in Fig. 3, evaluation of raw data in Table S2). That is, despite some anomalies, the relative errors of Sb_x and Sb_{tot} are not significantly different to zero (i.e., when $Sb_x = Sb_{tot}$), and there is no statistical difference between the relative errors of MGTS I and MGTS III (i.e., *t*-tests, Fig. 3). Therefore, this variability of ±15 % is attributed to analytical precision, supported by the statistical analyses of the datasets via Tukey 25th - 75th quartiles and analysis of atypical values, performed with the software IBM SPSS v20 (Table S2). If an analytical variability of 9 % was applied (i.e., repeatability tests from Lacanau samples, $N = 8$, Table 1) there would be a systematic bias towards negative relative differences for MGTS I (i.e., intermediate discharge conditions, $Sb_x > Sb_{tot}$ concentrations) and positive relative differences for MGTS III (i.e., low discharge conditions, $Sb_x < Sb_{tot}$ concentrations). Given the common extreme, positive and negative anomalies for both hydrological conditions (Fig. 3), such a systematic bias seems unlikely, thus we consider that 9 % and 15 % relative differences are in the same order of magnitude. However, negative anomalies ($Sb_x > Sb_{tot}$ concentrations, beyond the - 15 % threshold) are counter intuitive given the definition of Sb_x and Sb_{tot}, thus can only be attributed to UV treatment contributions. It is possible that inefficient UV treatment occurred in some samples, increasing the reactivity of Sb organic compounds, causing losses during analyses via ICP-MS (e.g., adsorbing onto the tubes). Positive anomalies ($Sb_x < Sb_{tot}$ concentrations, beyond the +15 % threshold) occur during both hydrological conditions at $S > 15$ (Table S2). This effect could be caused by the presence of organo-Sb species (e.g., methylstibonic acid-MSA and/or dimethylstibinic acid-DMSA, Andreae, 1983) or Sb-NOM complexes <0.2 μm in estuarine water samples, as Sb stable anionic forms ($Sb(OH)_3$ and $Sb(OH)_6^-$) at natural water pH are not readily complexed with dissolved organic matter (van den Berg et al., 1991). However, some of the positive anomalies could also be explained by the effect of Teflon bottles during UV treatment, as evidenced from Milli-Q® Millipore blanks (i.e., 0.15 ± 0.13 nM or 18.8 ± 16.4 ng L^{-1}, raw data in Table S1). Overall, only one study has directly quantified the influence/presence of ~10 % organic-Sb species in estuarine systems (i.e., at $S > 15$ in the Ochlockonee River estuary, Andreae et al., 1981), and two studies in coastal waters (Bertine and Lee, 1983; Gillain and Brihaye, 1985) accounting for over 30 % of the total Sb dissolved concentrations (Filella et al., 2002a; Filella and Rodríguez-Murillo, 2021). Therefore, the presence of organic species or complexes contributing to the observed, positive differences between Sb_x and Sb_{tot} cannot be ruled out, though more evidence is required to quantify the proportion of organo-Sb species in the Gironde Estuary and validate this hypothesis.

3.3. Reactivity in the Gironde Estuary

Dissolved Sb along the salinity gradient of the Gironde Estuary showed variable concentrations ranging between 0.82 nM (100 ng L^{-1}) in the freshwater endmember to 3.61 nM (440 ng L^{-1}) in mid-salinities, obtaining 1.64 nM (200 ng L^{-1}) for the seawater endmember (Fig. 4a,b). The results on Sb endmembers are consistent with previous studies in the freshwater ranges of the fluvial Gironde Estuary. That is, the freshwater endmembers match known median concentrations of 1.31 ± 0.41 nM (160 ± 50 ng L^{-1}) at La Réole (2003–2016; Gil-Díaz et al., 2018) and, even more precisely, with the corresponding concentrations of the sampling month: ~0.82 nM (~100 ng L^{-1}) in MGTS I (Fig. 4a) and ~1.15 nM (~140 ng L^{-1}) in MGTS III (Fig. 4b). Likewise, the seawater endmembers at the estuary mouth, and those from the Arcachon Bay water used in repeatability tests, are also in accordance with literature average seawater concentrations of 1.51 ± 0.37 nM (184 ± 45 ng L^{-1};

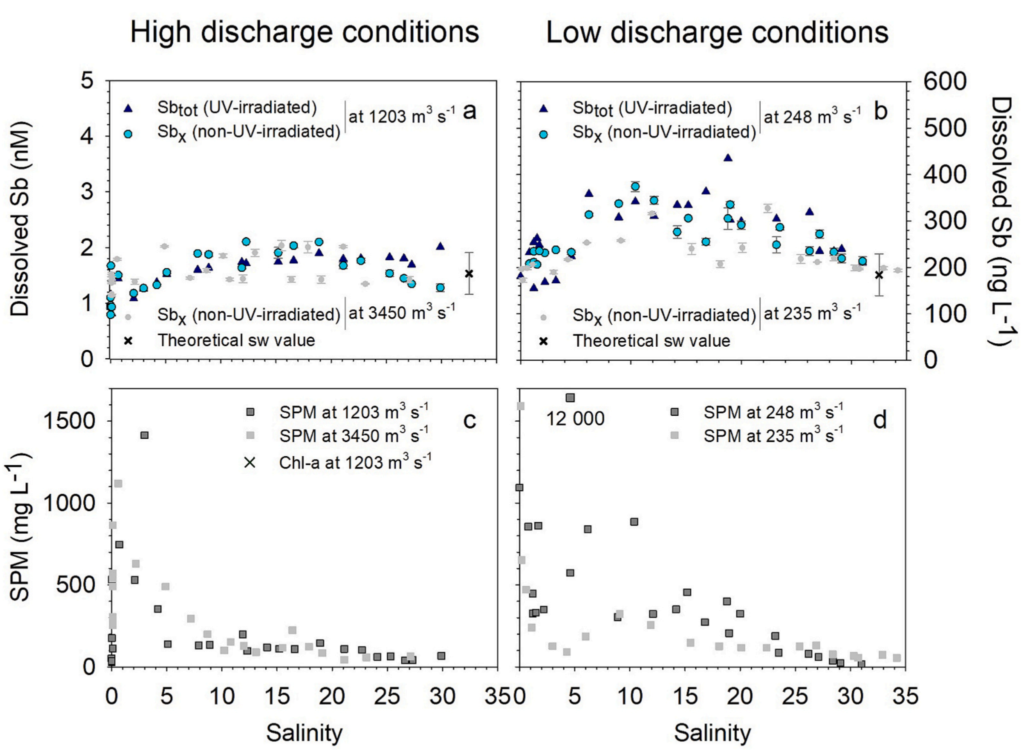

Fig. 4. Geochemical profiles along the salinity and turbidity gradients of the Gironde Estuary. Distribution of antimony (Sb; a,b) dissolved concentrations, as well as suspended particular matter (SPM; c,d) along the salinity gradient of the Gironde Estuary during intermediate/high (MGTS I - 1203 $m^3 s^{-1}$ and MGTS II - 3450 $m^3 s^{-1}$; a,c) and low (MGTS III - 248 $m^3 s^{-1}$ and MGTS IV - 235 $m^3 s^{-1}$; b,d) freshwater discharges. Both non-UV-irradiated samples (Sb_x; filled circles) and UV-irradiated replicates (Sb_{tot}; filled triangles) are represented when applicable. Error bars (in grey) show standard deviations of total Sb concentrations from individual isotope standard additions. The theoretical range of 1.51 ± 0.37 nM (184 ± 45 ng L^{-1}, cross; Filella et al., 2002a) for seawater is also included.

Filella et al., 2002a).

However, Sb trends along the salinity gradient suggest that the reactivity of Sb in the Gironde Estuary is complex. That is, Sb reactivity shows an additive behavior that varies in intensity with contrasting hydrological conditions (i.e., there are statistically significant differences between Sb concentrations in MGTS I and MGTS III, Fig. S2). During intermediate discharge conditions (1203 $m^3 s^{-1}$, Fig. 4a), Sb_{tot} doubles its freshwater concentration between $0 < S < 10$ and then remains stable at 1.64 nM (~200 ng L^{-1}). A similar trend was observed in the Tamar River estuary, a macrotidal estuary with a defined MTZ of max. 3 g L^{-1} and observed anoxic conditions (van den Berg et al., 1991), i.e., similar hydrological characteristics than the Gironde Estuary. In the Tamar River, the rapid Sb increase at $S < 10$ was explained as a particle release effect from the MTZ or a redox release from interstitial waters. Therefore, given that this Sb behavior appears at different salinity ranges, it seems that there is an additive release of Sb related to common intra-estuarine biogeochemical processes of macrotidal MTZ-dominated estuaries, other than pure effects from the salinity gradient. This is in accordance with the little evidence on Sb environmental chloro-complexation for both Sb(III) and Sb(V) species in seawater (Filella et al., 2002b).

During low water discharge conditions (248 $m^3 s^{-1}$ and 235 $m^3 s^{-1}$, Fig. 4b), Sb_{tot} showed a reproducible desorption/dilution bell-shape behavior along the salinity gradient of the Gironde Estuary. More precisely, Sb showed an M-shaped distribution along the salinity gradient, with maximum concentrations at $S \sim 10$ and $S \sim 22$ (Fig. 4b). Similar M-shaped patterns have been observed in the Scheldt Estuary and the Savannah Estuary. The Scheldt Estuary is also a macrotidal estuary with a MTZ of 400 mg L^{-1} and an oxygen maximum zone at low S, i.e., approaching Gironde Estuary drought conditions where average 100–300 mg L^{-1} Suspended Particulate Matter (SPM) are present along the salinity gradient. The Scheldt Estuary only presented M-shaped Sb_d distributions during a sampling campaign in September 1982 and not in other winter campaigns during February 1975 and October–November 1978 (van der Sloot et al., 1985). Likewise, the Savannah Estuary is a mesotidal continent-ocean transition system presenting reducing conditions, with also maximum Sb concentrations at $S \sim 10$ and $S \sim 22$ for a sampling campaign during June 1986 (Byrd, 1990). Therefore, the same estuary can present different Sb reactivity trends along the salinity and turbidity gradients according to intra-estuarine seasonal dynamics.

Noteworthy, Byrd (1990) compared Sb concentrations to SPM, oxygen levels and inorganic nitrogen (i.e., nitrate + nitrite + ammonia concentrations) along the Savannah Estuary salinity gradient. He observed a decrease of Sb from the freshwater endmember to $S \sim 2.5$, related to Sb removal by association with iron flocculating colloids or a source variation effect and then explains the observed M-shape as follows: (i) a first Sb increase at $S \sim 10$ matching the lowest oxygen saturation and maximum nitrogen concentrations, i.e., related to organic matter remineralization or redox-conditioned Sb solubilization from SPM, (ii) a consequent decrease until $S \sim 17$ related to water column mixing, and (iii) a second Sb increase at $S \sim 22$ matching also a second inorganic nitrogen peak, i.e., suggesting a common link/source between Sb and the nitrogen cycle, before (iv) being quickly removed or diluted towards the seawater endmember. In fact, open ocean studies have also observed increased Sb concentrations in inorganic nitrogen rich areas like in upwelling systems, suggesting biotic uptake in surface waters and regeneration in depth (Cutter and Cutter, 1995). Thus, our results could suggest that the decrease in Sb at $S \sim 17$ can correspond to Sb sorption onto SPM (Fig. 4d) and/or a transformation into organo-Sb species (see Section 3.2.), potentially from biofilm or periphyton microorganisms during low discharge conditions (Fig. 4b). In any case, additional parameters such as chlorophyll-a and phaeopigments (Fig. S1) do not provide any insights to clarify this hypothesis, thus further, complementary information (e.g., NO_3^- concentrations) should be collected in future field campaigns.

Overall, our contrasting results between hydrological conditions are complementary, as they suggest that during intermediate conditions only the first Sb maximum dominates inside the estuary, migrating to mid-salinity ranges (Fig. 4a). This agrees with previously detected influences of estuarine water and SPM residence times in Sb reactivity in the Gironde Estuary (Gil-Díaz et al., 2016). Indeed, long residence times match low freshwater discharges promoting suboxic conditions in the water column. This, in turn, favors the development of reducing conditions (Robert et al., 2004) which can reduce redox-sensitive carrier phases such as amorphous iron oxyhydroxides, potentially releasing particulate Sb to the dissolved phase in the main first Sb peak. This can be observed more precisely by the decrease in Th-normalized particulate Sb concentrations from fluvial to estuarine reaches presented in the next section (Table 2).

3.4. Dissolved net fluxes to the Atlantic coast

Daily fluxes of gross fluvial income to the estuary and net estuarine coastal output can be calculated for the studied sampling campaigns according to the methods described in Boyle et al. (1974) and Andreae et al. (1983). These methods require multiplying average daily freshwater discharges to the river endmember (C*) and the "effective" river (C^0) concentrations, respectively. Gross fluxes are calculated from the Sb C* whereas net fluxes are determined from the Sb C^0, that is, the extrapolation of the Sb physical dilution trend indicated by the data from the seawater endmember to $S = 0$. Such values can be calculated from dissolved Sb distributions along the salinity gradient (as shown in Supplementary data, Fig. S3). Our results (Table 2) show Sb_d freshwater endmember variability (C*) from high concentrations in summer/low discharges (MGTS III/IV) to low concentrations in winter/high discharges (MGTS I/II) in accordance with already observed river seasonal patterns in the Garonne River (Gil-Díaz et al., 2018). These results also show that the observed non-conservative behavior in the estuarine salinity gradient is not a reflection of seasonal fluvial variability (C*). Such case would only be possible if C* showed the same concentration as C^0 (Andreae et al., 1983) and this is neither achieved for the sampling periods nor during the previous months before the sampling campaigns, as registered in the database at La Réole from Gil-Díaz et al. (2018). However, the latter only considers the contribution from the Garonne River, and further studies should include the influence of the Dordogne and Isle rivers (Fig. 1). Thus, estimated "effective" concentrations (C^0) reflect the effect of residence time and Sb dissolution kinetics during intra-estuarine reactivity.

Despite more intense Sb reactivity during drought than intermediate discharge conditions (i.e., higher bell-shapes during low discharge conditions, Fig. 4b), (i) net fluxes are highly dominated by water discharges and, in the end, (ii) similar particulate fluvial inputs (Sb/Th ~ 0.20) result in common estuarine downstream concentrations (Sb/Th ~ 0.16) for all sampling campaigns (Table 2). In fact, the average release of Sb into the dissolved phase inside the estuary during low discharge conditions accounted for ~0.05 ± 0.02 kmol Sb d^{-1} (~ 6.22 ± 2.42 kg Sb d^{-1}), whereas intermediate discharges increased to ~0.14 kmol Sb d^{-1} (~ 16.6 kg Sb d^{-1}), and flood conditions doubled to ~0.28 kmol Sb d^{-1} (~ 34.0 kg Sb d^{-1}). These results suggest that (i) intra-estuarine Sb_p release into the dissolved phase is either very fast, or (ii) there is a long-term influence of SPM accumulation in the MTZ (i.e., given the SPM residence times of up to 2 years, Castaing and Jouanneau, 1979) homogenizing seasonal effects in the particulate phase compared to the observations in the dissolved phase, and or (iii) there is a (yet unaccounted) relevant role of the Dordogne/Isle rivers into Sb_d fluxes that would leverage the differences between the gross and net fluxes (i.e., as, given the sampling stations in this work, the value from the freshwater endmember only shows the contribution of the Garonne River).

Compared to other continent-ocean transition systems, the observed daily flux dissolution in the Gironde Estuary is lower than that registered for the Tagus Estuary in April 1982 (Andreae et al., 1983). In fact, the Tagus Estuary is a highly polluted mesotidal estuary presenting a

Table 2
Estimated Sb river concentration (C*), "effective" river Sb concentration (C^0) and respective gross and net fluxes for MGTS I - IV sampling campaigns in the Gironde Estuary. Corresponding Th-normalized (Sb/Th) Sb particulate average concentrations (± SD) at the freshwater endmember (La Réole; Gil-Díaz et al., 2016) and estuarine reaches (S > 20, Gil-Díaz et al., 2016) are also shown.

Campaign	Discharge $m^3\ s^{-1}$	C* nM *(ng L^{-1})*	C^0 nM *(ng L^{-1})*	Gross flux kmol d^{-1} *(kg d^{-1})*	Net flux kmol d^{-1} *(kg d^{-1})*	Fluvial Sb/Th	Estuarine Sb/Th
MGTS I (March 2014)	1203	0.82 *(100)*	2.14 *(260)*	0.09 *(10.4)*	0.22 *(27.0)*	0.19 ± 0.01	0.15 ± 0.00
MGTS II (March 2015)	3450	0.85 *(103)*	1.78 *(217)*	0.25 *(30.7)*	0.53 *(64.7)*	0.22 ± 0.01	0.16 ± 0.03
MGTS III (October 2015)	248	1.31 *(160)*	4.35 *(530)*	0.03 *(3.4)*	0.09 *(11.4)*	0.20 ± 0.02	0.16 ± 0.01
MGTS IV (June 2017)	235	1.13 *(138)*	2.96 *(360)*	0.02 *(2.8)*	0.06 *(7.3)*	0.20 ± 0.01	0.15 ± 0.04

maximum of dissolved inorganic Sb between 28 < S < 32 of ~5.75 nM (~700 ng L^{-1}), explaining the 0.47 kmol Sb d^{-1} (57 kg Sb d^{-1}) release into the dissolved phase for average water discharges of 181 $m^3\ s^{-1}$. Less populated areas, however, like that in the Waikato River show similar orders of magnitude for the dissolved Sb gross fluxes than those observed in the Gironde fluvial system, averaging 0.12 kmol Sb d^{-1} (15 kg Sb d^{-1}) for average water discharges of ~200 $m^3\ s^{-1}$ throughout the whole year (2006–2008, Wilson and Webster-Brown, 2009). Nevertheless, the seasonal variability detected for the gross fluxes in the Gironde Estuary (i.e., ranging from 2.8 to 30.7 kg Sb d^{-1}) is larger than that observed in the Waikato River (i.e., ranging from ~8.5 to ~19.0 kmol Sb d^{-1}, Wilson and Webster-Brown, 2009). In any case, the Sb net fluxes calculated here are non-negligible, as they show similar orders of magnitude (e.g., MGTS I) and even 4-fold higher fluxes (e.g., MGTS III) than those calculated for cadmium during the same sampling campaigns (Pougnet et al., 2021), i.e., the main historical contaminant in the Gironde Estuary (Dabrin et al., 2009).

4. Conclusion

Overall, this work provides guidelines for good analytical quantification of Sb in challenging water matrices, improving current and future understanding of Sb biogeochemical cycles in continent-ocean transition systems.

Given the lack of estuarine/seawater CRM for dissolved Sb, results show a better analytical performance of the QQQ-ICP-MS technique, validating its use for direct routine analyses of dissolved Sb in brackish/seawater matrices. Direct quantification of acidified water samples (Sb_x) alone can be considered as a general good approach for total Sb concentrations (i.e., UV pre-treatment can introduce artifacts). Thus, we report for the first time since the year 2000, analytically sound values for the Atlantic seawater endmember, agreeing with the established range identified in Filella et al. (2002a). Furthermore, QQQ-ICP-MS efficiently removes site-dependent interferences, though their identity has not yet been identified for the Gironde Estuary mouth. This means that, other estuarine systems might show similar, yet unidentified, site-dependent effects, which can be easily verified/addressed by collecting coastal water samples nearby the study site, not influenced by the estuarine system.

Updated profiles of the non-conservative behavior of Sb in the Gironde Estuary allow to confidently calculate daily net/gross fluxes, highlighting a geogenic/natural predominance of Sb reactivity in the area, sensitive to complex redox and biological processes. This reactivity seems independent of major chloro-complexing effects, contrary to other trace elements like cadmium (Dabrin et al., 2009) or silver (Lanceleur et al., 2013), and shows a seasonal variability, characteristic of specific estuarine morphologies and hydrodynamics. This means that Sb reactivity is not stationary and that future works on estuarine systems should sample more than once in a lifetime (no more single campaigns, as evidenced in the literature), reporting several parameters including the month of sample collection, water discharges, SPM/nutrient load and residence times, whenever possible.

CRediT authorship contribution statement

Teba Gil-Díaz: Writing – review & editing, Writing – original draft, Visualization, Methodology, Investigation, Formal analysis, Data curation, Conceptualization. **Frédérique Pougnet:** Writing – review & editing, Writing – original draft, Project administration, Investigation. **Lionel Dutruch:** Writing – review & editing, Investigation. **Jörg Schäfer:** Writing – review & editing, Supervision, Resources, Funding acquisition. **Alexandra Coynel:** Writing – review & editing, Validation, Resources, Project administration, Funding acquisition, Conceptualization.

Declaration of competing interest

None.

Data availability

The raw data of this study will be made available upon request.

Acknowledgements

This study contributes to the AMORAD Project (ANR-11-RSNR-0002) from the National Research Agency, allocated in the framework program "Investments for the Future" and has benefited from support by the ANR Program Adapt'Eau (ANR-11-CEPL-008), the European Community and the Region Aquitaine (FEDER Aquitaine-1999-Z0061), as well as the EU FP7 Ocean 2013.2 Project SCHeMA (Project-Grant Agreement 614002). The authors greatly acknowledge support from "l'Agence de l'Eau Adour-Garonne" and to the crew of the French Oceanographic R/V Thalia (sampling campaigns MGTS I doi 10.17600/14008300 and MGTS III doi 10.17600/15010600).

Appendix A. Supplementary data

Supplementary data to this article can be found online at https://doi.org/10.1016/j.marchem.2024.104465.

References

Abdou, M., Gil-Díaz, T., Schäfer, J., Catrouillet, C., Bossy, C., Dutruch, L., Blanc, G., Cobelo-García, A., Massa, F., Castellano, M., Magi, E., Povero, P., Tercier-Waeber, M. L., 2020. Short-term variations of platinum concentrations in contrasting coastal environments: the role of primary producers. Mar. Chem. 222, 103782. https://doi.org/10.1016/j.marchem.2020.103782.

Andreae, M.O., 1983. The determination of the chemical species of some of the "hydride elements" (arsenic, antimony, tin and germanium) in sea water: methodology and results. In: Wong, C.S., Boyle, E., Bruland, K.W., Burton, J.D., Goldberg, E.D. (Eds.), Trace Metals in Sea Water. Springer Science + Business, Media New York. https://doi.org/10.1007/978-1-4757-6864-0_1.

Andreae, M.O., Asmode, J.F., Foster, P., Van't Dack, L., 1981. Determination of antimony (III), antimony (V), and methylantimony species in natural waters by atomic absorption spectrometry with hydride generation. Anal. Chem. 53 (12), 1766–1771. https://doi.org/10.1021/ac00235a012.

Andreae, M.O., Byrd, J.T., Froelich, P.N., 1983. Arsenic, antimony, germanium and tin in the Tejo Estuary, Portugal: modeling a polluted estuary. Environ. Sci. Technol. 17, 731–737. https://doi.org/10.1021/es00118a008.

Balaram, V., 2021. Strategies to overcome interferences in elemental and isotopic geochemical analysis by quadrupole inductively coupled plasma mass spectrometry: a critical evaluation of the recent developments. Rapid Commun. Mass Spectrom. 35 (10), e9065.

Bertine, K.K., Lee, D.S., 1983. Antimony content and speciation in the water column and interstitial waters of Saanich inlet. In: Wong, C.S., Boyle, E., Bruland, K.W., Burton, J.D., Goldberg, E.D. (Eds.), Trace Metals in Sea Water. NATO Adv. Res. Inst. Plenum Press, New York, pp. 21–38. https://doi.org/10.1007/978-1-4757-6864-0_2.

Billy, I., Oriol, L., Mousseau, L., Passafiume, O., 2015. Détermination de la chlorophylle a par fluorimétrie. Procédure : protocole national chlorophylle a. SOMLIT.

Boyle, E., Collier, R., Dengler, A.T., Edmond, J.M., Hg, A.C., Stallard, R.F., 1974. On the chemical mass-balance in estuaries. Geochim. Cosmochim. Acta 38, 1719–1728. https://doi.org/10.1016/0016-7037(74)90188-4.

Byrd, J.T., 1990. Comparative geochemistries of arsenic and antimony in rivers and estuaries. Sci. Total Environ. 97 (98), 301–314. https://doi.org/10.1016/0048-9697(90)90247-R.

Caplette, J.N., Mestrot, A., 2021. Chapter 11 Biomethylation and Biovolatilization of Antimony. De Gruyter, Antimony, Berlin, Boston, pp. 251–274. https://doi.org/10.1515/9783110668711-011.

Castaing, P., Jouanneau, J.M., 1979. Temps de résidence des eaux et des suspensions dans l'estuaire de la Gironde. J. Recherche Océanographie IV 41–52.

Castelle, S., 2008. Spéciation et réactivité du mercure dans le système fluvio-estuarien girondin. Doctoral dissertation. Université de Bordeaux. Available from INIS: http://inis.iaea.org/search/search.aspx?orig_q=RN:51092023.

Cutter, G.A., Cutter, L.S., 1995. Behavior of dissolved antimony, arsenic and selenium in the Atlantic Ocean. Mar. Chem. 49, 295–306. https://doi.org/10.1016/0304-4203(95)00019-N.

Dabrin, A., Schafer, J., Blanc, G., Strady, E., Masson, M., Bossy, C., Castelle, S., Girardot, N., Coynel, A., 2009. Improving estuarine net flux estimates for dissolved cadmium export at the annual timescale: application to the Gironde estuary. Estuar. Coast. Shelf Sci. 84, 429–439. https://doi.org/10.1016/j.ecss.2009.07.006.

DFG (Deutsche Forschungsgemeinschaft), 2023. MAK- und BAT-Werte-Liste. VCH, Weinheim. https://doi.org/10.34865/mbwl_2023_deu.

European Commission (EU COM474), 2020. Critical Raw Materials for Strategic Technologies and Sectors in the EU. Document. available at: https://rmis.jrc.ec.europa.eu/uploads/CRMs_for_Strategic_Technologies_and_Sectors_in_the_EU_2020.pdf (Last accessed: 31st January 2024).

European Council (EC), 2006. Directive 2006/11/EC of 15 February 2006 on pollution caused by certain dangerous substances discharged into the aquatic environment of the community. OJ L64/52.

Filella, M., Rodríguez-Murillo, J.C., 2021. Chapter 9 From headwaters to oceans: antimony across the aquatic continuum. In: Antimony. De Gruyter, Berlin, Boston, pp. 191–230. https://doi.org/10.1515/9783110668711-009.

Filella, M., Belzile, N., Chen, Y.W., 2002a. Antimony in the environment: a review focused on natural waters I: occurrence. Earth Sci. Rev. 57, 125–176. https://doi.org/10.1016/S0012-8252(01)00070-8.

Filella, M., Belzile, N., Chen, Y.W., 2002b. Antimony in the environment: a review focused on natural waters II: relevant solution chemistry. Earth Sci. Rev. 59, 265–285. https://doi.org/10.1016/S0012-8252(02)00089-2.

Filella, M., Belzile, N., Lett, M.C., 2007. Antimony in the environment: a review focused on natural waters III. Microbiota relevant interactions. Earth Sci. Rev. 80 (3–4), 195–217. https://doi.org/10.1016/j.earscirev.2006.09.003.

Fu, X., Xie, X., Charlet, L., He, J., 2023. A review on distribution, biogeochemistry of antimony in water and its environmental risk. J. Hydrol. 625 (B), 130043. https://doi.org/10.1016/j.jhydrol.2023.130043.

Gil-Díaz, T., Schäfer, J., Pougnet, F., Abdou, M., Dutruch, L., Eyrolle-Boyer, F., Coynel, A., Blanc, G., 2016. Distribution and geochemical behavior of antimony in the Gironde estuary: a first qualitative approach to regional nuclear accident scenarios. Mar. Chem. 185, 65–73. https://doi.org/10.1016/j.marchem.2016.02.002.

Gil-Díaz, T., Schäfer, J., Coynel, A., Bossy, C., Dutruch, L., Blanc, G., 2018. Antimony in the lot-Garonne River system: a fourteen-year record of solid/liquid partitioning and fluxes. Environ. Chem. 15 (3), 121–136. https://doi.org/10.1071/EN17188.

Gillain, G., Brihaye, C., 1985. A routine speciation method for a pollution survey of coastal sea-water. Oceanol. Acta 8 (2), 231–235.

Guérin, T., Chekri, R., Vastel, C., Sirot, V., Volatier, J.L., Leblanc, J.C., Noël, L., 2011. Determination of 20 trace elements in fish and other seafood from the French market. Food Chem. 127 (3), 934–942. https://doi.org/10.1016/j.foodchem.2011.01.061.

Kuznetsova, O.V., Timerbaev, A.R., 2021. Direct seawater analysis by high-resolution ICP-MS provides insights into toxic metal accumulation in marine sediments. At. Spectrosc. 42, 85–90. https://doi.org/10.46770/AS.2021.005.

Lanceleur, L., Schäfer, J., Blanc, G., Coynel, A., Bossy, C., Baudrimont, M., Glé, C., Larrose, A., Renault, S., Strady, E., 2013. Silver behavior along the salinity gradient of the Gironde estuary. Environ. Sci. Pollut. Res. 20, 1352–1366. https://doi.org/10.1007/s11356-012-1045-3.

Li, H., Tong, R., Guo, W., Xu, Q., Tao, D., Lai, Y., Jin, L., Hu, S., 2022. Development of a fully automatic separation system coupled with online ICP-MS for measuring rare earth elements in seawater. RSC Adv. 12 (37), 24003–24013. https://doi.org/10.1039/D2RA02833F.

Lorenzen, C.J., 1967. Determination of chlorophyll and pheo-pigments: spectrophotometric equations. Limnol. Oceanogr. 12, 343–346. https://doi.org/10.4319/lo.1967.12.2.0343.

Mitra, A., Sen, I.S., 2017. Anthrobiogeochemical platinum, palladium and rhodium cycles of earth: emerging environmental contamination. Geochim. Cosmochim. Acta 216, 417–432. https://doi.org/10.1016/j.gca.2017.08.025.

Pougnet, F., 2018. Etat de la qualité des eaux de l'estuaire de la Gironde : cas du cadmium et des butylétains. In: Biodiversité et Ecologie. Université de Bordeaux, Français. NNT: 2018BORD0011. tel-01773964v2. https://theses.hal.science/tel-01773964v2.

Pougnet, F., Blanc, G., Mulamba-Guilhemat, E., Coynel, A., Gil-Díaz, T., Bossy, C., Strady, E., Schäfer, J., 2021. Nouveau modèle analytique pour une meilleure estimation des flux nets annuels en métaux dissous. Cas du cadmium dans l'estuaire de la Gironde. Hydroécologie Appliquée. 21, 47–69. https://doi.org/10.1051/hydro/2019002.

Pougnet, F., Gil-Díaz, T., Blanc, G., Coynel, A., Bossy, C., Schäfer, J., n.d. not published. Historical mass balance of cadmium decontamination trends in a major European continent-ocean transition system: case study of the Gironde Estuary. Mar. Environ. Res. 176, 105594. doi:10.1016/j.marenvres.2022.105594.

Robert, S., Blanc, G., Schäfer, J., Lavaux, G., Abril, G., 2004. Metal mobilization in the Gironde Estuary (France): the role of the soft mud layer in the maximum turbidity zone. Mar. Chem. 87, 1–13. https://doi.org/10.1016/S0304-4203(03)00088-4.

Salaün, P., Gibbon-Walsh, K.B., Alves, G.M., Soares, H.M., van den Berg, C.M., 2012. Determination of arsenic and antimony in seawater by voltammetric and chronopotentiometric stripping using a vibrated gold microwire electrode. Anal. Chim. Acta 746, 53–62. https://doi.org/10.1016/j.aca.2012.08.013.

Siems, A., Zimmermann, T., Sanders, T., Pröfrock, D., 2024. Dissolved trace elements and nutrients in the North Sea—a current baseline. Environ. Monit. Assess. 196 (6), 539. https://doi.org/10.1007/s10661-024-12675-2.

Tamás, M.J., 2016. Cellular and molecular mechanisms of antimony transport, toxicity and resistance. Environ. Chem. 13 (6), 955–962. https://doi.org/10.1071/EN16075.

U.S. Environmental Protection Agency, 2013. Priority pollutant list. In: Appendix A, 40 Code of Federal Regulations 423. http://www.gpo.gov/fdsys/pkg/CFR-2013-title40-vol30/xml/CFR-2013-title40-vol30-part423.xml. Last accessed on the 18/07/2015.

van den Berg, C.M., 1993. Complex formation and the chemistry of selected trace elements in estuaries. Estuaries 16 (3), 512–520. https://doi.org/10.2307/1352598.

van den Berg, C.M.G., Khan, S.H., Daly, P.J., Riley, J.P., Turner, D.R., 1991. An electrochemical study of Ni, Sb, Se, Sn, U and V in the Estuary of the Tamar. Estuar. Coast. Shelf Sci. 33, 309–322. https://doi.org/10.1016/0272-7714(91)90059-K.

van der Sloot, H.A., Hoede, D., Wijkstra, J., Duinker, J.C., Nolting, R.F., 1985. Anionic species of V, As, Se, Mo, Sb, Te and W in the Scheldt and Rhine estuaries and the southern bight (North Sea). Estuar. Coast. Shelf Sci. 21, 633–651. https://doi.org/10.1016/0272-7714(85)90063-0.

Vernon, L.P., 1960. Spectrophotometric determination of chlorophylls and Pheophytins in plant. Extracts Anal. Chem. 32, 1144–1150. https://doi.org/10.1021/ac60165a029.

Wilson, N., Webster-Brown, J., 2009. The fate of antimony in a major lowland river system, the Waikato River, New Zealand. Appl. Geochem. 24 (12), 2283–2292. https://doi.org/10.1016/j.apgeochem.2009.09.016.

Wu, F., Zheng, J., Pan, X., Li, W., Deng, Q., Mo, C., Zhu, J., 2008. Prospect on biogeochemical cycle and environmental effect of antimony. Adv. Earth Science 23 (4), 350. https://doi.org/10.11867/j.issn.1001-8166.2008.04.0350.

Wu, X.D., Song, J.M., Li, X.G., Yuan, H.M., Li, N., 2011. Behaviors of dissolved antimony in the Yangtze River Estuary and its adjacent waters. J. Environ. Monit. 13 (8), 2292–2303. https://doi.org/10.1039/C1EM10239G.

Yentsch, C.S., Menzel, D.W., 1963. A method for the determination of phytoplankton chlorophyll and phaeophytin by fluorescence. Deep-Sea Res. Oceanogr. Abstr. 10, 221–231. https://doi.org/10.1016/0011-7471(63)90358-9.

Yost, R.A., 2022. The triple quadrupole: innovation, serendipity and persistence. J. Mass Spectrom. Adv. Clin. Lab 24, 90–99. https://doi.org/10.1016/j.jmsacl.2022.05.001.

Zhu, Y., 2020. Determination of rare earth elements in seawater samples by inductively coupled plasma tandem quadrupole mass spectrometry after coprecipitation with magnesium hydroxide. Talanta 209, 120536. https://doi.org/10.1016/j.talanta.2019.120536.

Zhu, Y., Ariga, T., Nakano, K., Shikamori, Y., 2021. Trends and advances in inductively coupled plasma tandem quadruple mass spectrometry (ICP-QMS/QMS) with reaction cell. At. Spectrosc. 42, 299–309. https://doi.org/10.46770/AS.2021.710.